

Full Length Research

Impact of land use change on surface runoff and stream discharges in Luvuvhu River Catchment

Singo, L.R. *, Kundu, P.M. and Odiyo, J.O.

University of Venda, Department of Hydrology and Water Resources, Private Bag, X5050,
Thohoyandou, 0950, South Africa

Accepted 30 June, 2016; Published 30 July, 2016

Luvuvhu River catchment in Limpopo Province of South Africa experiences floods resulting from heavy rainfall of intensities exceeding 15 mm per hour associated with the Intertropical Convergence Zone. The generation of runoff is triggered by the rainfall intensity and soil moisture status. Runoff was calculated as a product of the net precipitation and a curve number coefficient. It was then routed using the Muskingum-Cunge method through the basin along flow paths determined by the topography using a diffusive wave transfer model that enabled the calculation of response functions between start and end point, depending upon slope, flow velocity and dissipation characteristics along the flow lines. Results showed that the simulated discharges closely compared with the measured discharges without the need for model optimization. It was concluded that simulation techniques had the potential to determine the influence of changes in land use to the hydrologic response of the catchment.

Key words: Catchment, digital elevation model, hydrological model, routing, runoff

INTRODUCTION

The Luvuvhu River catchment experiences floods resulting from heavy rainfall associated with the Intertropical Convergence Zone (ITCZ). Land cover degradation in the catchment is a major cause of environmental concern in Limpopo Province. The headwaters are gradually getting depleted due to uncontrolled anthropogenic activities by the rising human population. Lack of appropriate land and water management strategies lead to land degradation by soil erosion, increased runoff and sedimentation processes during rainfall events (DWAF, 2003). It is therefore imperative that studies to investigate, detect and quantify the land cover changes and their potential impact on the hydrological processes be carried out to provide baseline information for management purposes.

Advances in earth observation and GIS techniques have broadened the scope of global data acquisition, providing the capacity to quantify and estimate spatially

distributed hydrological processes (Moore *et al.*, 1991; Carpenter *et al.*, 1999). Satellite sensors including Landsat 7 ETM+, SPOT 4, MODIS, MERIS and NOAA among others now provide repetitive land surface data and have made it possible to quantify multitemporal variability of land cover (Coppin *et al.*, 2004). Hydrogeophysical catchment parameters can be derived from the global digital soil and topographic datasets after which, computer-based hydrological models are applied to solve complex hydrological problems.

In order to analyse flood flow, distributed channel flow routing models employ convective diffusion equations to estimate flow characteristics at various stages within the river channel. River stage or flow rates are required for the design and evaluation of hydraulic structures. Most river reaches in the study area are ungauged and a methodology is needed to estimate rates of flow at specific locations in streams where no measurements are available. Flood routing techniques are utilised to estimate the stages in order to predict flood wave propagation along river reaches. Models can be developed for gauged catchments and their parameters

*Corresponding author. Email: rhinah.singo@gmail.com

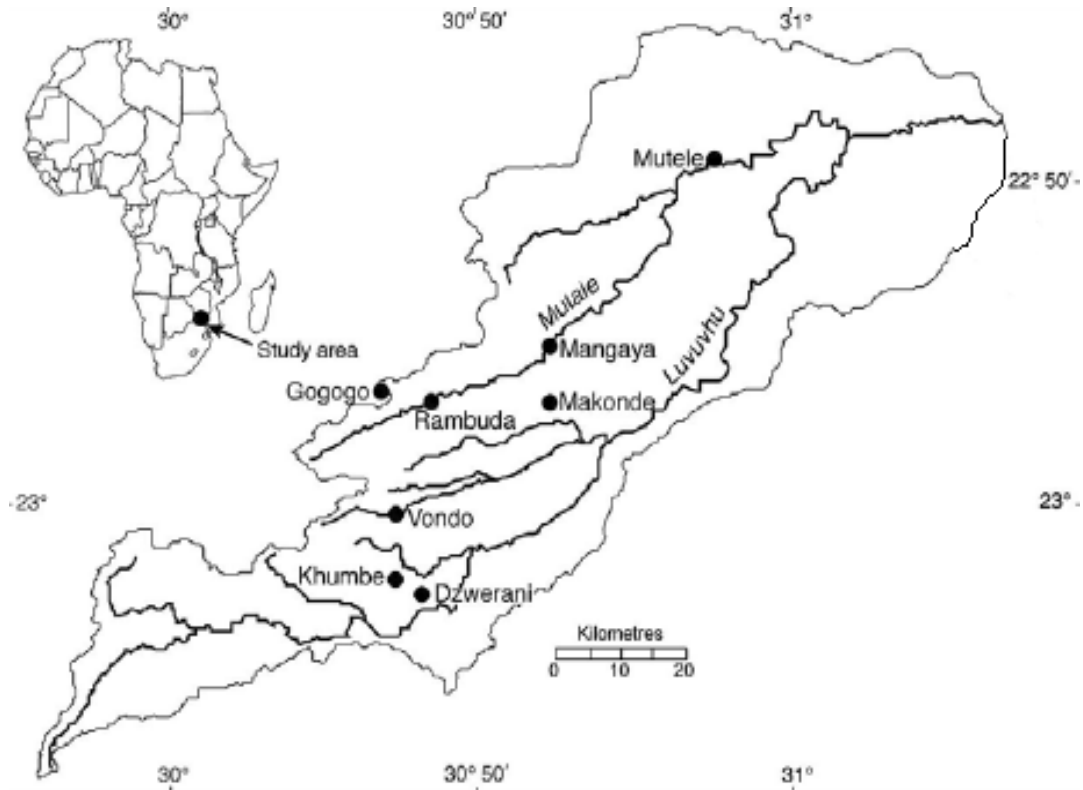


Figure 1. The Study Area.

related to physical characteristics such as slope, reach width, reach length so that the approach can be applied to ungauged catchments in the neighbouring regions. These models are more demanding in data requirement and computational time limiting their application in rural rivers with data constraints. Lumped flow routing models estimate the momentum effects of flow based on empirical relationships of storage and discharge but depending on the lumping scale used, the application of these models can sometimes lead to loss of vital hydrological information. In this study, the Muskingum-Cunge equation was used to evaluate the effects of land cover changes on flood volumes and peak discharges. Hydrological models for runoff generation, transformation and channel flow routing were applied for simulations using semi-distributed modeling techniques.

The Luvuvhu River catchment shown in Figure 1 is located in Limpopo Province in northeastern South Africa, between latitudes $22^{\circ}17'34''\text{S}$ and $23^{\circ}17'57''\text{S}$ and longitudes $29^{\circ}49'46''\text{E}$ and $31^{\circ}23'32''\text{E}$, and covers an area of about 5941 km^2 . It lies at the periphery of the southernmost position of the ITCZ during the summer with average January position at about 15°S . The climate of the area is largely influenced by the ITCZ, modified by local orographic effects. Rainfall distribution in the catchment is classified as unimodal, having a rainy season predominantly between the months of October to

January with the average annual rainfall of about 200-400mm. The predominant soils in upland areas are Leptosols while the lowlands are dominated by Vertisol and Acrisols with Regosols dominating the lowveld. Generally, the catchment exhibits diverse land use/land cover patterns that are influenced by seasonality and socio-cultural practices of the local communities. Land use practises largely vary from plantation forests interspersed with large scale macadamia and banana plantations in the headwaters interspersed with small farm holdings for subsistence agriculture.

METHODS

Land cover and land use change

Land cover changes were detected and quantified through classifications of Landsat Multispectral Scanner (MSS) images, Landsat Thematic Mapper (TM) images and Landsat Enhanced Thematic Mapper (ETM+) images. To minimize distorting spectral characteristics caused by mosaicking multi-date images before classification, the scenes were independently classified. The images were first resampled to a common spatial resolution of 80m using the nearest neighbor interpolation technique. The predominant land cover classes selected

for the study included agriculture, forest, grassland, shrubland, wetland and water. To obtain consistent land cover, classes for semi-distributed hydrological modeling, a per-pixel image classification approach was adopted where the images were classified based on guided clustering as described by Yuan *et al.* (2005). The accuracy of the quantified land cover changes was determined using the standard measures for assessing the accuracy of remotely sensed data referred to as the overall accuracy and the kappa index (Congalton and Green, 1999).

A majority filter was applied to remove isolated pixels arising out of the classification. The images were then converted into vector coverages which were used to derive the required land cover statistics within the derived sub-catchments. Topological and morphometric characteristics of the catchment were derived from the global digital elevation model developed by the Shuttle Radar Topographic Mission (SRTM). Tiles at a spatial resolution of 90 m by 90 m were obtained in GeoTiff image format, pre-processed and later registered. A Digital Elevation Model (DEM) was subsequently resampled to a nominal pixel resolution of 80 m by 80 m using the bilinear interpolation technique and hydrologically corrected through a DEM burn-in procedure and sink removal. The sub-catchments, stream network and their morphometric properties were derived from the dataset in a GIS based on the standard procedures that simulate flow directions and accumulation as described by Moore *et al.* (1991) and Burrough and McDonell (1998).

Land use change was assessed using two time windows where the 1980's were taken as the period before change, and the 2000's as the period after change. A statistical sampling methodology based on Area Frame Sampling (AFS) was adopted to determine land use change. The unaligned systematic random sampling technique was preferred in order to capture representative samples of the heterogeneous land use in the catchment. The samples were chosen based on one square kilometer fixed size ground segments which have been found to be the most bias-free sampling design (Berry and Baker, 1968). A 1 km x 1 km grid corresponding to the 1:50,000 map sheet was overlaid upon the images, after which the locations of ground segments were chosen randomly from each block. Each segment had unique and identifiable boundaries outlined on images and maps. By the method of direct expansion (Cochran, 1977; Allen and Hanuschak, 1988; Taylor and Eva, 1992; Sushil, 2001) the area for each land use and land cover class was determined for the entire study area.

Soil data

Digital soil data at a scale of 1:2Million, were acquired

from the Global Environment Facility Soil Organic Carbon database for the SADC countries. This dataset was an upgraded version developed by national experts from the global Soil and Terrain (SOTER) database. Soil data were reclassified into the major hydrological soil groups (HSG) of the catchment with the help of FAO/UNESCO revised manual for soil maps of the world based on their drainage characteristics. The World Reference Base for Soil Resources (WRB) classification (FAO-ISRIC-ISSS, 1998) was used as a unifying medium of communication.

Hydrometeorological analysis

Rainfall and stream flow data between the period of 1960 and 2014 for the selected pluviometric stations located in the catchment were obtained from the Department of Water Affairs (DWA) and South African Weather Services (SAWS). GIS tools in ArcGIS were used to create layers for the various data sets including the catchment boundary, stream lines and the meteorological stations. Spatial analysis was carried out to determine stream patterns, longest flow paths, average slopes, time of concentration and catchment orientation. The flood frequency for the period of over 50 years was analysed using Gumbel's (1941) extreme value method shown in equation 1, which is more appropriate for obtaining better outcomes for larger extrapolations of flood data.

$$P(X \geq X_0) = 1 - e^{-e^{-y}} \quad (1)$$

where: P = the probability of occurrence, X = the event of the hydrologic series, x_0 = the desired value of the event, y = the reduced variate $y = \alpha(X - \beta)$, x = the variate value.

Event based simulations were carried out where three typical storm events were selected and used as input to the rainfall-runoff models. To assess the impact of the land cover changes, synthetic storm events of varying magnitudes assumed to be uniformly distributed and with the same duration in the sub-catchments were selected for scenario analysis. The storm events were applied at nominal depths to the different land cover conditions to investigate the possible effects on the floods, based on the analyzed trends of the rainfall records acquired.

Models and parameterization

The hydrological models which were adopted included the Natural Resource Conservation Service-Curve Number (NRCS-CN), Clark's Unit Hydrograph (C-UH), and the Muskingum-Cunge flow routing models available within the HEC HMS (HEC, 2000). Transformation of the runoff into corresponding hydrographs at the outlet of the catchment was achieved using the

Clark's Unit Hydrograph (UH) concept (USACE, 1994). The time of concentration was estimated from the lag time while the storage coefficient was estimated using a procedure which relates the parameter to the time of concentration and the geometrical properties of the catchment (Sabol, 1988). The exponential recession and empirically fitted parameter model was used to represent baseflow processes. The model required the determination of the recession constant and the initial baseflow, which was approximated from the baseflow trends during periods of high flow. Routing of the channel flow was performed using the Muskingum-Cunge hydrologic model shown in equation 2 (Cunge, 1969; HEC, 2000). Estimates for the bank full depth, width of the river channel bottom and other flow characteristics were acquired from the DWA.

$$Q_{j+1}^{n+1} = C_1 Q_j^n + C_2 Q_j^{n+1} + C_3 Q_{j+1}^n + C_4 Q_L \quad (2)$$

where,

$$C_1 = \frac{\frac{\Delta t}{k} + 2x}{\frac{\Delta t}{k} + 2(1-x)} \quad C_2 = \frac{\frac{\Delta t}{k} - 2x}{\frac{\Delta t}{k} + 2(1-x)}$$

$$C_3 = \frac{2(1-x) - \frac{\Delta t}{k}}{\frac{\Delta t}{k} + 2(1-x)} \quad C_4 = \frac{2\left(\frac{\Delta t}{k}\right)}{\frac{\Delta t}{k} + 2(1-x)}$$

where: C_1, C_2, C_3, C_4 = model coefficients, k = travel time of wave through the reach, Δt = change in time, x = shape parameter, I = inflow, L = Lateral flow

The length of the river reaches and their slopes were derived from the DEM using Geo-HMS and the GIS script for HEC HMS. The channel geometry at every reach of study and the Manning's roughness coefficient were estimated from field observations of the reaches and river bed materials using the method described by Cowan (1956).

Curve number estimates for antecedent moisture conditions were obtained from standard curve number tables where estimates for agricultural land use were used and later adjusted into antecedent moisture condition (AMC) III, prevalent during floods. The calculated curve numbers were obtained using Equations 3 and 4.

$$Q = \left(\frac{(P - I_a)^2}{P - I_a + S} \right) \quad (3)$$

where, Q = runoff (mm); P = rainfall (mm); I_a = initial abstraction (mm); S = potential maximum retention after runoff begins (mm).

Based on experiences from previous studies, the initial abstraction was assumed to be 20% of the maximum potential retention (S), which was related to the mean curve number parameter, CN_m by:

$$S = \frac{25400}{CN_m} - 254 \quad (4)$$

RESULTS

Land cover and land use change

There was significant land cover change from forestland, woodland and open grassland to large scale farms, medium size farms, subsistence agriculture and built-up land as shown in Figures 2 and 3. It was observed that hills around Tshakuma and Tsianda which were covered by natural forest in the pre-change period were largely covered by small portions of trees and bushes at higher levels, interspersed agriculture at the middle and built up, mixed with agroforestry on hill-sides. The notable farms within the catchment were Levubu, Tsianda and Piesanghoek while the expanded built up area was around the greater Thohoyandou and Elim.

Area estimation by direct expansion

The results obtained by direct expansion and regression estimation were as shown in Table 1. At the level of individual classes, the best results by both ground survey and image classification were obtained for bananas with a coefficient of variation of 10.22% and a regression coefficient of 5.07%. This could be due to the structure of the banana plant where the broad leaves provided a smooth texture and tone hue that gave a distinct feature class under supervised classification. The other crops and tree plantations had smaller leaves which provided mottled structure and poor tone hue that led to mixed and sometimes unidentifiable classes on imagery. The eucalyptus plantations had the lowest reliability with a coefficient of variation of 70.65. This could be due to the mixed reflectance from fire corridors and the contiguous woodlots and tree crops such as avocados, guavas and macadamia. The error matrices developed to assess the accuracies of the classifications indicated values between 78-86% for the overall accuracy, and 65-80% for $Kappa$ index. These values were used as the measure of actual agreement, and the expected output in the sense that values within these ranges normally indicated good representations of the actual land use and land cover.

Based on secondary data, the results showed that

Forest/Woodland between 1980 and 2013

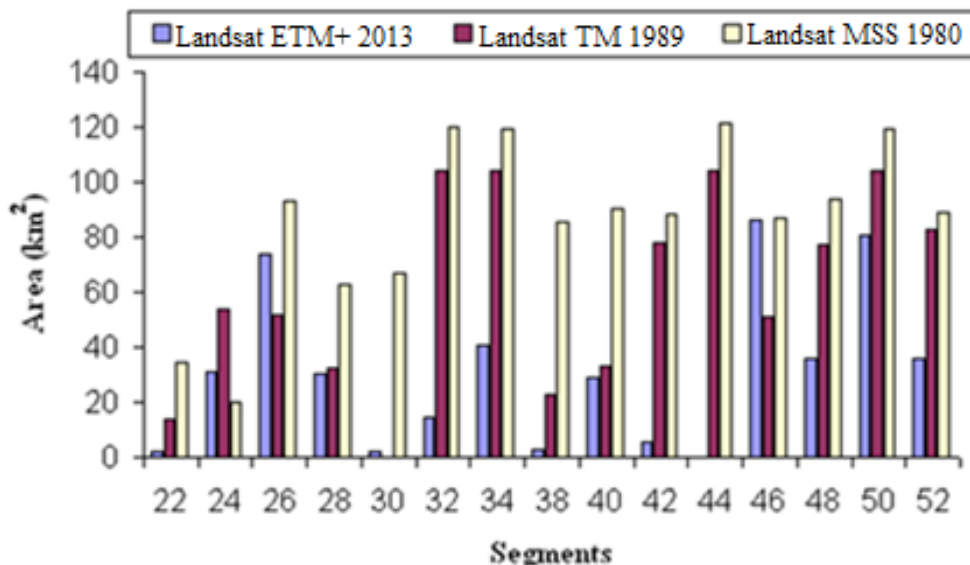


Figure 2. Forest and Woodland between 1980 and 2013.

Arable Land between 1980 and 2013

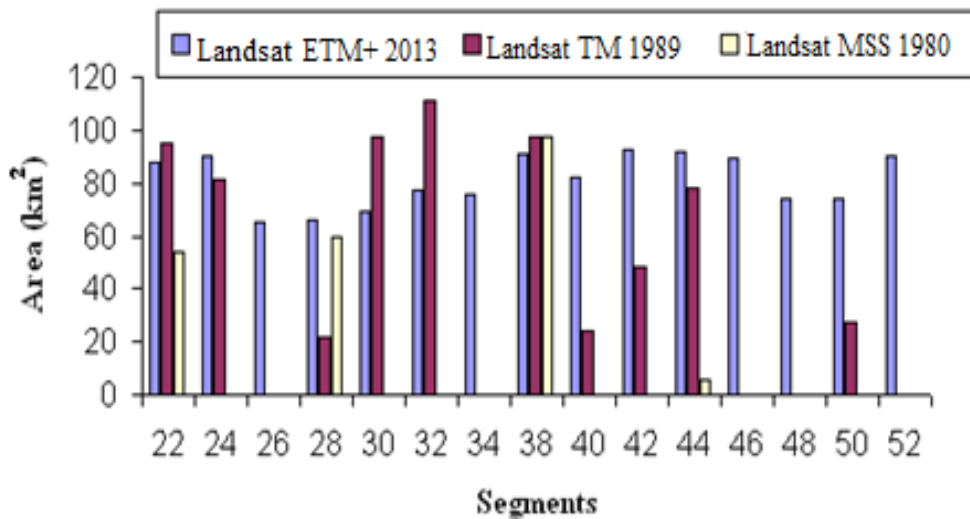


Figure 3. Arable land between 1980 and 2013.

during the 80's, land cover patterns constituted of 15.81% agriculture, 29.34% natural forest, 32.15% bare ground, 0.06% water bodies, 8.28% plantations and 14.36% shrubs and grasses. During this period, natural forests and bare ground dominated the study area covering almost 60%. During the 90's, a decrease in forest cover was noted with a major increase in bare ground revealing

change in land use in the area. Forest cover declined from 29.34% to 16.8%. Notable was agriculture and bare ground which rose from 15.81% to 21.73% and from 32.15% to 37.16% respectively. The area covered by plantations also increased by about 1.7% from 8.28% to 9.93%. Insignificant change was noted in water bodies, shrubland and grassland.

Table 1. Land cover and land use statistics for 2011.

| Land cover and land use within segments | | Surface area (ha) | Variance | σ | CV | RE |
|---|-----------------------|-------------------|------------|----------|-------|-------|
| Maize | direct expansion | 1,352 | 2,815,101 | 1245 | 60.12 | |
| | regression estimation | 1,009 | 833,650 | 650 | 29.90 | 4.95 |
| Macadamia | direct expansion | 3,799 | 4,896,099 | 1989 | 58.85 | |
| | regression estimation | 3,298 | 899,795 | 918 | 30.52 | 5.08 |
| Bananas | direct expansion | 25,664 | 9,984,885 | 3170 | 10.22 | |
| | regression estimation | 28,727 | 2,369,960 | 1447 | 5.07 | 3.98 |
| Agroforestry | direct expansion | 3,144 | 581,419 | 893 | 30.53 | |
| | regression estimation | 2,945 | 286,655 | 623 | 25.22 | 1.95 |
| Eucalyptus | direct expansion | 2,005 | 1,887,722 | 155 | 70.65 | |
| | regression estimation | 2,442 | 52,354 | 219 | 8.06 | 21.88 |
| Built up area | direct expansion | 12,558 | 15,554,215 | 3979 | 38.76 | |
| | regression estimation | 8,009 | 1,340,942 | 1255 | 18.32 | 15.11 |
| Grass/bushland | direct expansion | 30,550 | 16,868,711 | 3766 | 13.08 | |
| | regression estimation | 35,537 | 14,174,091 | 1473 | 11.74 | 2.90 |
| TOTAL AREA | | 61,072 | | | | |

In the post change period up to 2012, land use change revealed a decrease in natural forest from 32.15% to 20.675 and giving rise to agriculture which rose to 38.57%. An increase in water bodies from 0.06% to 0.08% was observed. This may be due to the construction of Nandoni dam which started operating in 2005 with the mandate to supply water to rural and peri-urban communities within the catchment. Originally, only Lake Fundudzi, Vondo dam and Albasini dams as well as some tributaries of Luvuvhu River were the dominant water bodies in the catchment.

Environmental monitoring in Luvuvhu River Catchment

By time series analysis of a sequence of images, which were available at 10-daily and monthly intervals and composed into annual data, the status and progress of vegetation and crop growing seasons were monitored. The data was analyzed by comparing historical images with current ones to show how rainfall was distributed over the areas as indicated by good or poor vegetation development. The annual Normalized Difference Vegetation Index (NDVI) image maps displayed the minimum to maximum greenness values attained at each pixel location over the period. The annual maximum of greenness typically occurred during the period of peak

vegetation of the primary growing season of a given year which therefore, revealed the level of greenness that would normally be expected at the peak of season. The minimum of the twelve annual maximums for any location generally represented the worst growing seasons of the nineteen year period. The trend analysis between rainfall and NDVI in Figure 4 showed a linear relationship where an increase in rainfall resulted in an increase in NDVI. In some cases, NDVI remained high during periods of no rainfall, meaning that temporal water shortage did not affect vegetation cover.

Rainfall- Runoff relationship

The long-term (1960-2014) average rainfall value of 1012.029 mm per annum was obtained for the catchment using the Thiessen Polygon method. In analyzing long term rainfall and runoff relationships, estimated values using curve numbers were related to variation in rainfall assuming the relationship between the two would be linear. The correlation obtained by linear regression was, $r^2 = 0.9739$, which represented a very significant direct relationship between the two parameters. The trend analysis of rainfall (Figure 5) showed that the annual rainfall differed across the catchment. Some stations displayed a decreasing trend while others showed increasing trends.

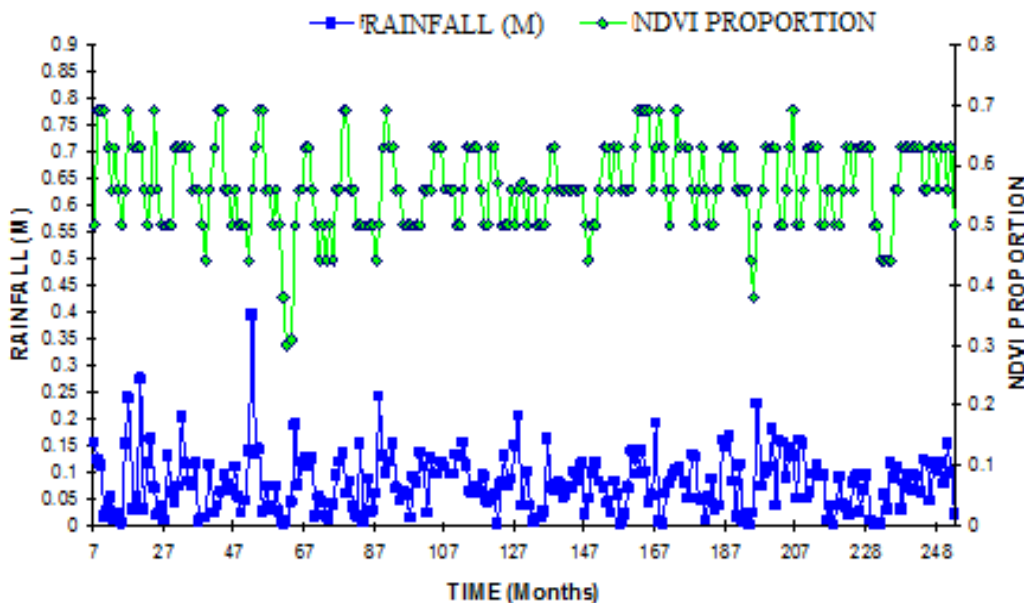


Figure 4. Monthly trends for rainfall and NDVI.

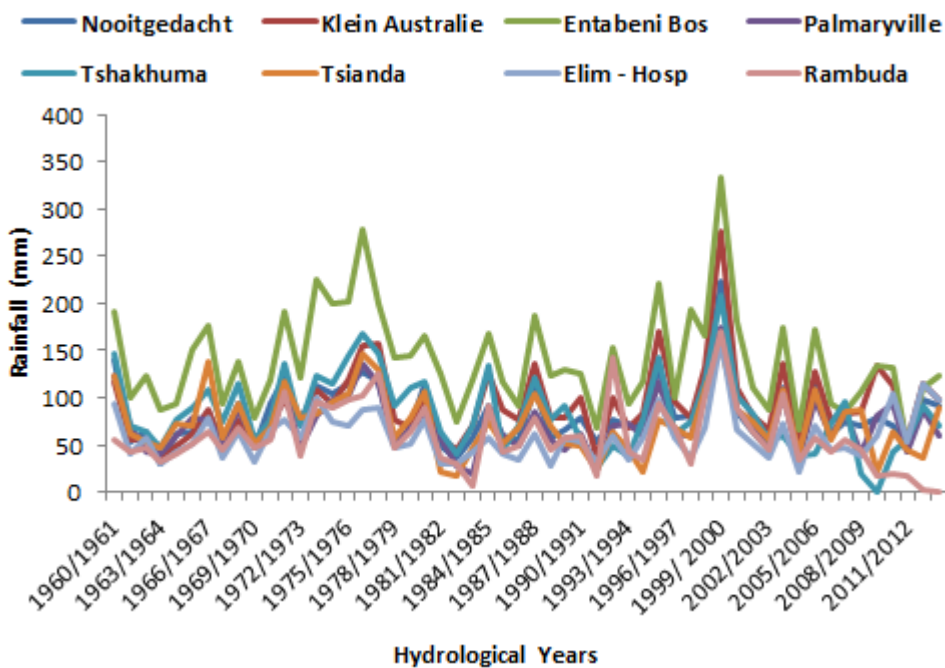


Figure 5. Rainfall trends.

The results showed that runoff was highly variable during the month of February with records of 16.3 m³ and 38.4 m³ upstream and downstream respectively. The results showed that upstream catchments had lesser amounts of runoff while abundance runoff volumes were received downstream of the catchment. Surface runoff during the 1960-1985 phase showed spatial and temporal variations. It can be noted from Figure 6 that runoff trends

at each gauging station varied from year to year and from place to place. Notable was the increase in runoff trends at A9H003 and A9H006 which were located upstream of the catchment. A slight increase at A9H015 and A9H016 and an unvarying trend at A9H020 downstream were noticed. A decrease in trends at A9H017 and A9H023 which were located downstream of the catchment was evident. Both trends revealed unimodal peaks centred

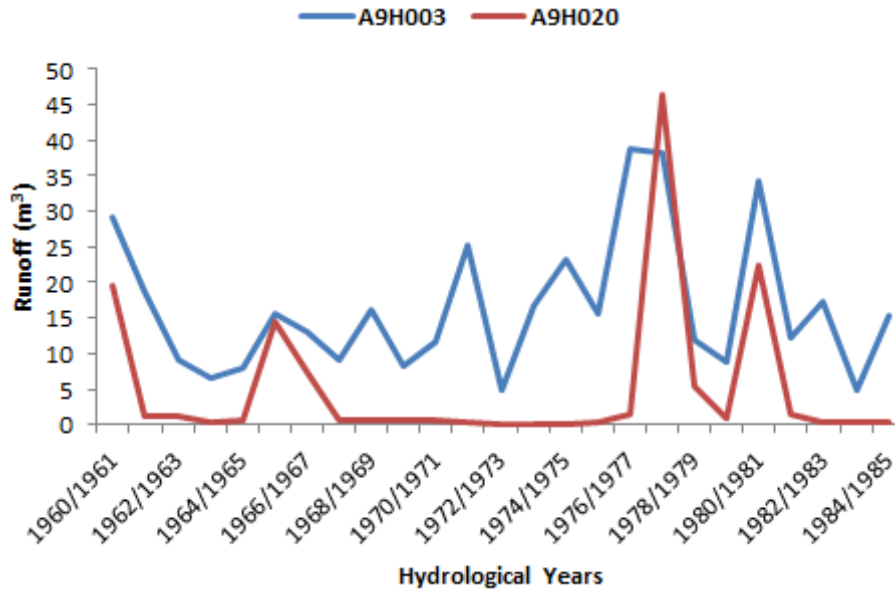


Figure 6. Runoff trends at A9H020 and A9H003 during the 1960-1985 phase

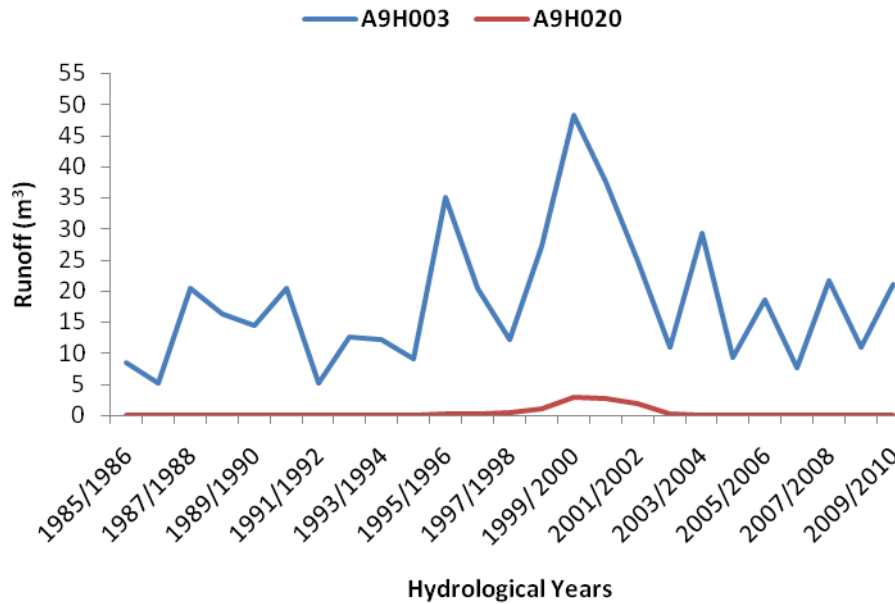


Figure 7. Runoff trends at A9H020 and A9H003 during the 1985-2010 phase.

around the hydrological year 1976/77 at A9H003 and A9H006; and hydrological year 1977/78 at A9H020; 1978/79 and at A9H016 and A9H023 respectively. During the dry periods of 1981/82 and 1982/83, stations A9H015 and A9H017 had record peak flow volumes while the rest of the catchment received little or no runoff. Appendix 9 showed runoff trends for various stations during the 1960 to 1985 period.

Trends in surface runoff during the 1985-2010 phase shown in Figure 7 indicated an increase in runoff downstream of the catchment. A hydrograph peak that

lasted for about 5 years was evident upstream of the catchment at station A9H020. During this phase, the station recorded erratic runoff trend between 1995/96 and 2002/03. Highest flood peak were recorded during 1996/97 both upstream and downstream of the catchment. However, runoff trends downstream of the catchment revealed greater variability. Trends in surface runoff at other stations revealed unimodal flow peaks at different hydrological years. Such peaks were recorded during 1996/97 at A9H015; 1999/2000; 2001/02 at A9H016; and 2003/04 at A9H006 and A9H017

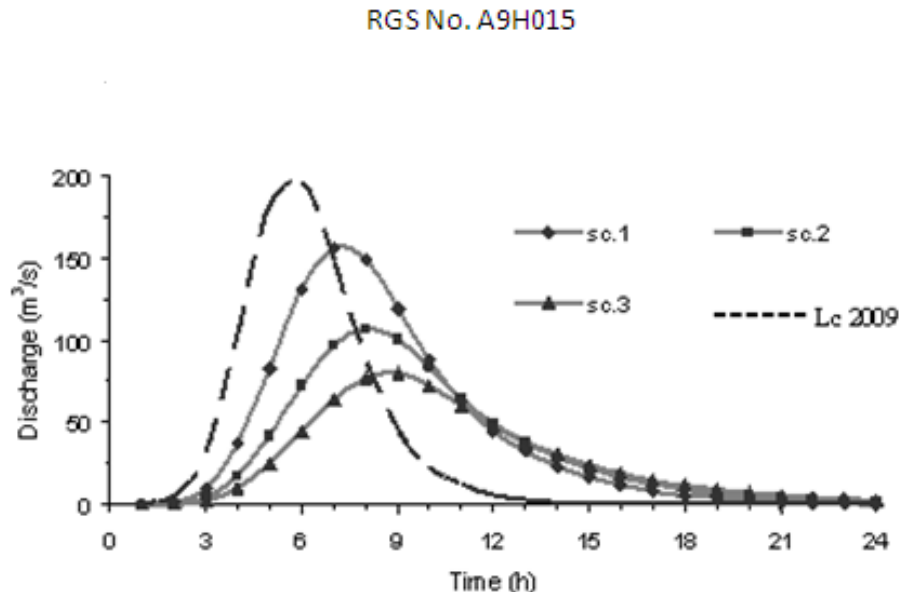


Figure 8. Flood hydrographs for the 50 mm synthetic storm event for the respective sub-catchments.

respectively, revealing spatial and temporal fluctuations in surface runoff in the study area.

Simulated runoff volumes

The flood hydrographs shown in Figure 8 illustrated how the three scenario analysis compared in terms of flood peak discharges and the associated volumes. The highest change in the runoff coefficient for the period of 1962-2009 was noted at RGS A9H015 located in the upstream of the catchment. During this period, the runoff coefficients increased in a similar way in the sub-catchments from 30 mm synthetic rainfall event. From the results, A9H015 sub-catchment for instance, produced peak discharges of 50 m³/s in 1980, 56 m³/s in 1989 and 65 m³/s in 2009. The runoff depths also increased over the same period. The sub-catchment draining at RGS A9H015 produced peak discharges of 117 m³/s, 140m³/s and 160 m³/s.

The simulated floods for the sub-catchment draining at RGS A9H015 conforms approximately to a normal flood event with a return period of 2 years in the catchment. From the results, peak discharges of 472 m³/s, 420 m³/s and 470 m³/s were obtained in 1980, 1989 and 2009 respectively. These values represented an increase of 20% between 1980 and 2009, with 11% occurring in the first period of 1980 and 1989. Also noted were the decreasing times to peak, with the same event in 1980 taking one hour more to reach the peak than in 2009. Flood volumes on the other hand increased by 11% over the entire period of study. The simulated flood event for January, 1984 conformed to a return period of about 10 years. Simulated peak discharges of 1517 m³/s, 1550 m³/s and 1750 m³/s were obtained for this event,

representing increases by 10%, 7% and 17% between 1980-1989, 1989-2009 and 1980-2009 respectively.

DISCUSSIONS

The use of multi-temporal remotely sensed data showed that Luvuvhu River Catchment had undergone significant changes in land cover over the decades. The satellite time series analysis of 1980 1989 and 2009 showed the pre-change and post-change cover types. An increase in population may have led to clearing of forests to make way of new activities in the area, such as agricultural fields and human settlements. Since the early 2000's, the government of South Africa implemented the Rural Development Programme (RDP) where the majority of natural forests were cleared to pave ways for human settlements leaving the area bare and susceptible to soil erosion.

The NRCS-CN related the detected land cover changes to the flood runoff using the physically derivable curve number parameter. Transformation of excess rainfall through the catchment was achieved using the Clark's Unit Hydrograph model, whose parameters were related to the derived composite curve number and morphometric characteristics of the catchment. The curve numbers assumed a linear relationship between rainfall and runoff which explained 97% of their variance. However, the analysis of stream flow showed that there was no direct relationship between rainfall and discharges. One could attribute it to the complex nature of land use in the area by the small holder farmers. It is possible that the overcrowded and congested land units carrying crops, woodlots, houses and grasses trap runoff without allowing infiltration and hence prevent it from

reaching the streams.

The trends during the 1960-1985 phase revealed an increase in rainfall upstream of catchment at Nooitgedacht and a decrease in rainfall downstream at Palmmaryville. Other stations which indicated an increasing trend included Klein Australie, Entabeni Bos, Tshakhuma and Rambuda. Three peaks were observed in 1976/77 at Palmmaryville and at Nooitgedacht in 1977/78, revealing the spatial and temporal fluctuations. A study by Mukheibir (2005) has shown that South African regions experience seasonal and interannual variations in rainfall. These variations have a great impact on the agricultural sector in the country. For example, the timing of rainfall during the onset of rainfall in October is crucial for planting of crops whereas the timing of rainfall in early February is crucial for the growth of crops (Jury *et al.*, 1997).

The simulated results indicated that the land cover changes affected the hydrological response of the basin leading to increased peak discharges and runoff volumes. This increase was more in the upstream sub-catchments where deforestation was rampant and led to dwindling soil moisture retention capabilities and rates of infiltration. The flood peak discharges in the whole basin was noted to have increased by at least 17% over the period of 1980 -2009. Changes in the peak discharges in the sub-catchments were also noted to decrease with increase in the rainfall amounts indicating the possibility that the land cover changes may not have a very strong influence during large storm events. The flood volumes were also noted to have increased by at least 11% over the same period of time. The flood time to peak indicated a decreasing trend, in the range of 0.5 to 1 hour within the years. Further investigations using a large number of observed rainfall events, and using a distributed hydrologic modeling approach should be adopted for the catchment.

ACKNOWLEDGEMENTS

The authors would like to acknowledge the support of the South African National Research Foundation (NRF) and the University of Venda for funding the study. We are grateful to relevant authorities at DWA and SAWS for providing valuable historical data

REFERENCES

- Allen, J.D., Hanuschak, G.A. (1988). The Remote Sensing Applications Program of the National Agricultural Statistics Service 1980-1987. National Agricultural Statistics Service staff report no. SRB-88-08. United States Department of Agriculture, National Agricultural Statistics Service.
- Berry, B.J.L. and Baker, A.M. (1968). Geographic sampling, Spatial Analysis: A Reader in Statistical Geography. (B.J.L. Berry and D.F. Marble, Eds.), Prentice Hall, Englewood Cliffs, N.J. pp. 91-100.
- Burrough, P.A. and McDonnell, R.A. (1998). Principles of Geographical Information System, Oxford University Press, New York.
- Carpenter, T.M., Sperflage, J.A., Georgakakos, K.P., Sweeney, T. and Fread, D.L. (1999). National threshold runoff estimation utilizing GIS in support of operational flash flood warning systems. *Journal of Hydrology*, 224(1-2): 21-44.
- Cochran, W.G. (1977). Sampling Techniques, 3rd Ed., John Wiley and Sons, Inc., New York.
- Congalton, R.G. and Green, K. (1999). Assessing the Accuracy of Remotely Sensed Data. CRC Press, Boca Raton, Florida.
- Coppin, P., Jonckheere, I., Nackaerts, K. and Muys, B. (2004). Digital change detection methods in ecosystem monitoring: a review. *Int. J. Rem. Sens.* 25: 1565-1596.
- Cowan, W.L. (1956). Estimating hydraulic roughness coefficients. *Agr. Eng.* 37(7): 473-475.
- Cunge, J.A. (1969). On the Subject of a Flood Propagation Computation Method (Muskingum Method). *J. Hydra. Res.* 7(2): 205-230.
- DWAF, (2003). Levuvhu and Letaba Water Management Area. Overview of water resources availability and utilization. Department of Water Affairs and Forestry, Government of South Africa.
- FAO-ISSS-ISRIC, (1998). World reference base for soil resources. World Soil Resources Report No. 84. Rome.
- Gumbel, E.J. (1941). The return period of flood flows. *Ann. Math. Statist.* 12(2): 163-190.
- HEC, (2000). Hydrologic Modeling System-HEC-HMS: Technical Reference Manual. US Army corps of Engineers Hydrologic Engineering Center, Davis, California, USA.
- Moore, I.D., Grayson, R.B. and Ladson, A.R. (1991). Digital terrain modeling: a review of hydrological, geomorphological and biological applications. *Hydr. Proc.* 5: 3-30.
- Sabol, G.V. (1988). Clark unit hydrograph and r-parameter estimation. *J. Hydra. Eng.* 114(1): 103-111.
- Sushil, P. (2001). Crop area estimation using GIS, remote sensing and area frame sampling. *Int. J. App. Ea. Obs. Geoinf.* 3: 86-92.
- Taylor, J.C. and Eva, H.D. (1992). Regional Inventories on Beds, Cambs and Northants (UK), 1992-final report to CEC-JRC, Silsoe College ISBN 1 871564522, 70p.
- USACE, (1994). Flood Runoff analysis. Engineering Manual No. 110-2-1417. Washington. USA.
- World Soil Information (ISRIC), SOTER database (version 2.0). Retrieved on 20th March, 2011 from <http://www.isric.org>
- Yuan, F., Sawaya, K.E., Loeffelholz, B.C., Bauer, M.E. (2005). Land cover classification and changes analysis of the twin cities (Minnesota) Metropolitan Area by multitemporal Landsat remote sensing. *J. Rem. Sens. Env.* 98: 317-328.